

Measurement of Residual Stresses in Parts Created by Shape Deposition Manufacturing

N.W. Klingbeil, J.W. Zinn and J.L. Beuth
Department of Mechanical Engineering
Carnegie Mellon University
Pittsburgh, PA 15213

Abstract

Residual stress build-up is a concern in any solid freeform fabrication process involving successive deposition of uncured or molten material, due to differential contractions caused by solidification or curing. The most detrimental effect of residual stresses is typically part warping, which can lead to unacceptable losses in part tolerance. In many processes residual stress build-up is a fundamental barrier to the consistent manufacture of high-quality artifacts. In this paper, two methods of measuring residual stresses in parts created by Shape Deposition Manufacturing (SDM) with microcasting are described. First, a technique for measuring warping in deposited plate-shaped specimens is detailed, which can be used to determine residual stress resultants as well as to quantify gross effects of processing changes on residual stress magnitudes. Next, x-ray diffraction procedures are described by which residual stresses in deposited layers can be measured at discrete in-plane locations as a function of depth. Measured results for 308L stainless steel deposits determined from each method are interpreted in the context of residual stress modeling results obtained numerically in a separate research effort. The measured results provide insight into the effects on residual stress of both the material deposition path and the discrete droplet-by-droplet nature of the microcasting deposition process. The insights provided here may also be applicable to other processes involving successive material deposition.

Introduction

The motivating application for this work is Shape Deposition Manufacturing (SDM), a layered manufacturing technique under development at Carnegie Mellon University (Merz *et al.*, 1994) and Stanford University (Fessler *et al.*, 1996). The SDM process involves successive deposition of layers of material and CNC machining of each layer. Applications of SDM include the manufacture of parts that have multiple materials, complex geometries that cannot be machined by conventional methods, and embedded electronic components. An advantage of SDM is that it can directly create fully-dense metal parts using materials such as stainless steel, copper and invar. Fully-dense metallic materials can be deposited in SDM by a number of different techniques, including microcasting, welding and laser deposition. Microcasting involves deposition of macroscopic droplets (1/8"-1/4" in diameter) of molten metal, and is the method of material deposition for which residual stresses are investigated in this study.

As discussed by Prinz *et al.* (1995) and Amon *et al.* (1997), there are a number of processing, thermal and mechanical issues associated with SDM. One of the most fundamental issues is the generation of residual stress, which is inherent in any process involving molten material deposition. Residual stress can lead to warping and loss of tolerance in SDM artifacts, and can also significantly reduce the structural reliability of finished parts. Thermomechanical numerical modeling of residual stress generation in microcasting has been investigated previously at Carnegie Mellon University (Chin *et al.* (1996a), Chin *et al.* (1996b), Chin *et al.* (1995)). In the current study, measurements of residual stress in 308L stainless steel microcast deposits are investigated and the results are interpreted in the context of the numerical modeling. The goals of this work include a better understanding of residual stress distributions in microcast layers, as well as insight into the effects of changes in process parameters on residual stress generation.

Residual stress measurements are obtained in this work by two different methods. The first method is the measurement of warping strains and curvatures in deposited plate structures. Somewhat similar measurements of warping deflections in laser deposited beam-shaped specimens have been described previously by Fessler *et al.* (1996). The procedures for measuring warping in plate specimens are relatively straightforward, and the results can be used to determine residual stress resultants for comparison with the numerical modeling, as well as to investigate gross effects of process changes on residual stress generation. The second (and substantially more complicated) method is x-ray diffraction, which directly determines residual stresses at discrete in-plane locations and depths into the deposit. The two methods are sufficiently independent that they are discussed and related to the numerical modeling separately herein, after which the common observations and the utility of the two methods are summarized. Results from both methods indicate that residual stress distributions in fully dense deposits reflect the droplet-by-droplet nature of the microcasting process.

Warping Measurements

In this section, techniques are discussed for the experimental measurement of warping in plate-shaped deposits. The test configuration is shown in Figure 1. A high temperature biaxial

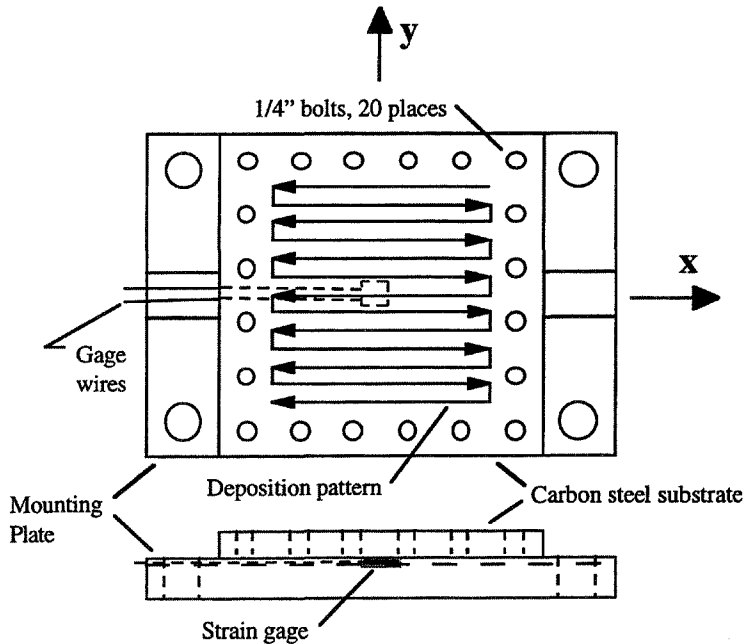


Figure 1. Warping Test Configuration

strain gage is centered on the bottom surface of a 6" x 6" x 1/2" fully-annealed 1018 carbon steel substrate. The steel substrate is then bolted near its edges to a 3/4" thick mounting plate, which is designed to allow for strain gage wires along the bottom of the substrate. The mounting plate is subsequently attached to a comparatively large pallet (not shown in Fig. 1) used in the SDM manufacturing process. The constraint of the pallet and mounting plate prevents warping of the specimen during manufacture. Material is then deposited in a 5" x 5" square onto the top surface of the substrate. For the test results discussed herein, the deposition path is as shown in Fig. 1, where the microcasting begins at the positive x,y corner and continues back and forth parallel to the x direction until ending in the negative x,y corner. Following material deposition, the specimen is allowed to cool to room temperature, and the deposit is machined flat to a thickness of 0.055". This thickness has been found by trial and error to render an essentially void-free deposit. Upon completion, the specimen is unbolted from the pallet and mounting plate, which results in residual

stress-induced warping. The resulting strains ϵ_x and ϵ_y in the x and y directions are recorded, and the warping deflections are measured using the coordinate measuring capabilities of the CNC milling machine (accurate to within $\pm 0.0005"$). Deflection measurements are taken at 81 equally-spaced points forming a 4.0" x 4.0" grid centered on the surface of the deposit.

Although the initial residual stress state results from high temperature nonlinear material response, the warping of finished specimens is dominated by elastic unloading. As a result, specimen warping can be interpreted in the context of linear elastic plate theory. The plate curvatures w_{xx} and w_{yy} in the x and y directions are estimated by quadratic curve fits of the measured deflections. In the event that the effects of in-plane shrinkage are small compared to bending, the measured strains ϵ_x and ϵ_y are proportional to the curvatures and supply redundant information. The bending stress resultants per unit width M_x and M_y are related to the curvatures w_{xx} and w_{yy} by the plate theory relations

$$M_x = \frac{EI}{1-v^2} (w_{xx} + vw_{yy}), \quad M_y = \frac{EI}{1-v^2} (w_{yy} + vw_{xx}), \quad (1)$$

where E is the elastic modulus, v is Poisson's ratio and I is the cross sectional moment of inertia per unit width. Application of eq. (1) assumes a negligible difference in elastic properties between the deposit and substrate, which is the case for stainless steel deposited onto carbon steel. Suitable relations for bending of layered plates composed of multiple dissimilar materials can be obtained as outlined by Pister and Dong (1952).

The procedures described above were used in obtaining sufficiently repeatable results for three specimens in which 308L stainless steel was microcast onto 1018 carbon steel substrates. A representative plot of measured specimen warping deflections is shown in Figure 2. Plots of the deflections taken through the center of the plate (along $y = 0$ and $x = 0$) are shown in Figure 3, from which quadratic curve fits were used to obtain the curvatures w_{xx} and w_{yy} in the x and y directions, respectively. A summary of the measured strains, curvatures and corresponding bending stress resultants for the three specimens is contained in Table 1. Note that the measured strains correspond well with the measured curvatures, indicating that the strains due to in-plane shrinkage are indeed small compared to the bending strains. Also, it is apparent from Table 1 that the calculated bending stress resultants M_x and M_y are relatively insensitive to variations in the measured curvatures, and are thus highly repeatable.

Some important insights into the effects of the material deposition path are evident from the test results. It is most noteworthy that for all three specimens, the strains and curvatures in Table 1 are larger in the x direction than in the y direction. In light of the deposition path shown in Fig. 1, this indicates that warping is more severe parallel to the direction of material deposition. This result suggests that for part geometries that are long in a particular direction, the maximum warping deflections might be reduced by depositing material in a path perpendicular to that direction. In addition, the curvature w_{xx} for the specimen of Fig. 2 was obtained as a function of y and was seen to decrease with decreasing values of y. In fact, the curvature w_{xx} at $y = -2.0"$ was 20% less than its value at $y = +2.0"$. Considering the deposition path of Fig. 1, it is apparent that warping in the direction of material deposition decreases as the total amount of deposited material increases. This result is in keeping with the expectation that substrate preheating occurring during material deposition tends to lessen the thermal mismatch, which ultimately leads to reduced warping. It is expected that alternative deposition paths could be used to achieve more uniform warping and/or reductions in part warping in critical directions.

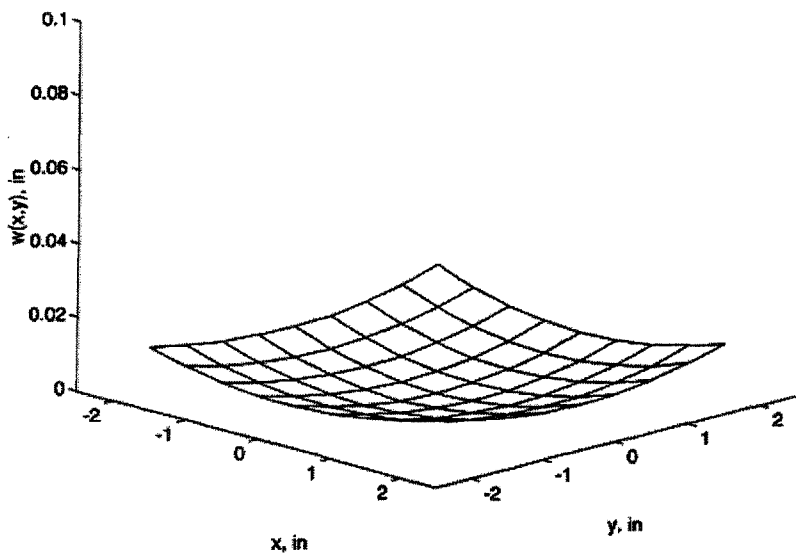


Figure 2. Measured Deflections for Specimen #1

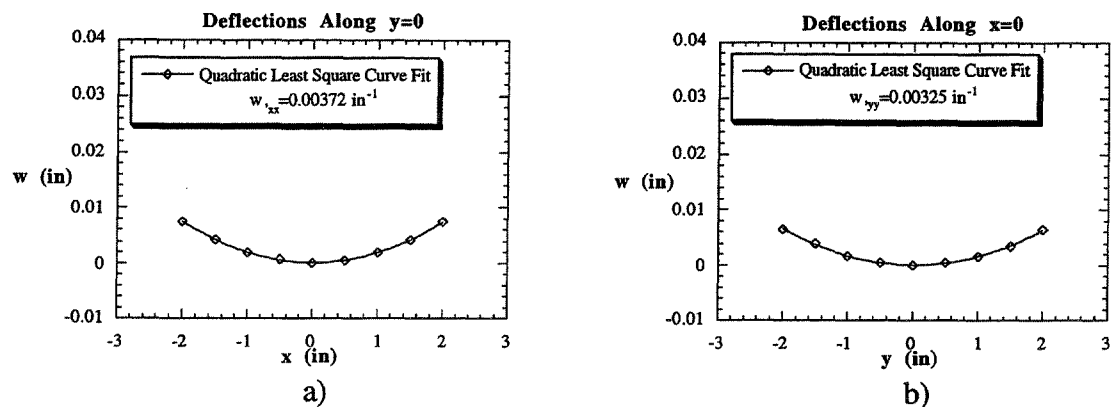


Figure 3. Quadratic Curve Fits for Specimen #1 Along a)y = 0 and b)x = 0

Table 1. Warping Test Results for Stainless Steel Microcast onto Carbon Steel

Specimen #	ϵ_x ($\mu\epsilon$)	ϵ_y ($\mu\epsilon$)	w_{xx} (in^{-1})	w_{yy} (in^{-1})	M_x ($\text{in} \cdot \text{lb/in}$)	M_y ($\text{in} \cdot \text{lb/in}$)
1	865	746	0.00372	0.00325	1.81×10^3	1.69×10^3
2	1010	697	0.00412	0.00295	1.93×10^3	1.62×10^3
3	931	703	0.00403	0.00322	1.93×10^3	1.71×10^3
Average Values	934	715	0.00395	0.00314	1.89×10^3	1.67×10^3

The warping measurements described above have been interpreted in the context of the 1-D thermomechanical residual stress modeling of Chin *et al.* (1996a). The 1-D results approximate the maximum residual stresses located along the centerline of a microcast droplet, away from the free edges. As a result, the 1-D results can be used to obtain an upper bound for the residual stress resultants corresponding to the case of an entire layer of material deposited at once. As discussed by Chin *et al.* (1996a), accurate high-temperature constitutive modeling is difficult, and the numerical results are merely estimates. However, 1-D numerical residual stress results for a geometry similar to that used in the experiments render a bending stress resultant equal to 3.94×10^3 in · lb/in, which corresponds to a curvature equal to 0.00681 in $^{-1}$ and a strain on the substrate bottom equal to 1860 $\mu\epsilon$. These values are on the order of twice the average measured values in Table 1. This result suggests that even in fully-dense microcast deposits, the effects of the droplet-by-droplet nature of the microcasting process are substantial, so that the average stress resultants are significantly less than those predicted by the 1-D model.

X-ray Diffraction Measurements

While plate warping measurements provide significant information regarding trends in residual stress resultants, they are unable to determine exact distributions of residual stresses in deposited layers. To this end, x-ray diffraction methods have also been used to measure residual stresses in deposited stainless steel. Determination of residual stress by x-ray diffraction is based on the measurement of changes in interplanar spacings between lattice planes in crystalline materials. In the interest of brevity, the details of x-ray diffraction theory are not addressed here. Background information on x-ray diffraction can be found in the book by Cullity (1978). The procedures for measurement of residual stress by x-ray diffraction are significantly more involved than those for measuring warping, and substantial care must be taken in both specimen preparation and calibration of the x-ray equipment. Standards for measurement of residual stress by x-ray diffraction include SAE J784a (1971) and ASTM E915-90 (1990).

In this study, a number of x-ray diffraction specimens were created to measure residual stress as a function of depth in microcast 308L stainless steel deposits. The results discussed in this section are for the specimen depicted in Figure 4. The specimen was cut from a larger deposit

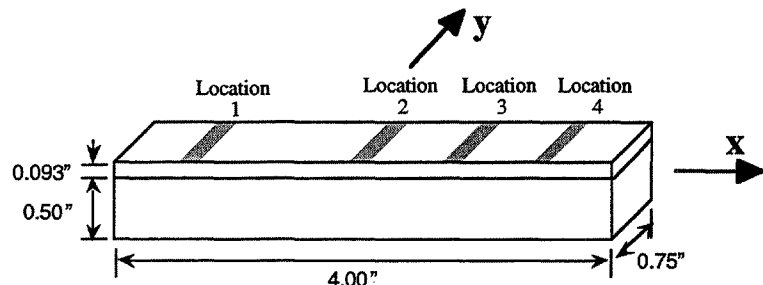


Figure 4. X-ray Diffraction Specimen Geometry

to in-plane dimensions of $0.75'' \times 4''$, with its length parallel to the direction of material deposition. The machined deposit surface was sanded, polished, and electropolished to remove all machining stresses. Electropolishing was conducted according to the guidelines in the *ASM Metals Handbook* (1973). Residual stresses parallel to the deposition direction were measured at 5 different depths into the deposited layer by removing thin layers of material through electropolishing. In order to investigate the possibility of local variations in residual stresses, results were obtained at 4 different locations along the length of the specimen.

Table 2 contains a summary of measured residual stresses at each depth for each location. As discussed in the previous section, a microcast deposit must be machined to roughly $0.055''$ in

order to be completely void free. In order to obtain stresses closer to the top of the deposit, this specimen was machined to a deposit thickness of approximately 0.0930" (which corresponds to a roughly 50% void-free surface) and then electropolished to Depth 1. Stresses were measured at Locations 1 and 3 for the first two depths, since these locations had no voids in the irradiated area. After the third depth, the specimen surface was over 80% void-free allowing stresses to be measured at Locations 1,2 and 4, which were more evenly spaced.

Table 2. X-ray Diffraction Measurements at Various Locations and Depths into the Deposit

Depth	Location 1		Location 2		Location 3		Location 4	
	Thickness,in	Stress,ksi	Thickness,in	Stress,ksi	Thickness,in	Stress,ksi	Thickness,in	Stress,ksi
Initial - 50% Voids	0.5915				0.5930			
Depth 1	0.5882	-95.6			0.5892	-58.6		
Depth 2	0.5871	-67.5			0.5880	-38.0		
Depth 3	0.5763	-21.5	0.5754	-33.3			0.5801	-45.0
Depth 4	0.5723	-10.6	0.5711	-8.56			0.5759	-25.8
Depth 5	0.5656	6.65	0.5647	15.9			0.5677	3.92

The general trend observed in the measured stresses at Locations 1, 2, 3, and 4, is that moving deeper beneath the surface of the deposit causes stresses to become more tensile and stress gradients to become less severe. Although there is some difference in stress magnitudes, there is generally good agreement between the stress gradients at the different locations. There is less in-plane variation in the measured stresses deeper into the deposit, which is likely due to the averaging of stresses by the overlapping of deposited droplets. The measured results indicate that there are two regimes of stress gradients in the deposit. Near the top of the deposit where high void concentrations exist, larger stress gradients of roughly -20,000 ksi/in are present. At greater depths where few voids are present, stress gradients of approximately -3,000 ksi/in are measured.

Figure 5 provides a plot of residual stresses as a function of depth at Location 1 as measured in the relaxed specimen and also as calculated for the same specimen with a bolted constraint. The bolted constraint on the substrate is modeled as a uniform edge moment, so that unbolting the substrate corresponds to the release of this moment. Thus, the stresses in the constrained deposit can be calculated by superimposing the measured stresses in the free specimen with the stresses produced by re-applying the released bending moment. The released moment M can be calculated from the curvature K using the beam-theory relationship $M = EIK$. A measured curvature equal to 0.005324 in^{-1} indicated a relaxed moment equal to $2082 \text{ in} \cdot \text{lb}$. Thus, bending stresses produced by a $2082 \text{ in} \cdot \text{lb}$ moment were added to the stresses measured in Layer I to obtain the stress distribution in the constrained specimen.

In addition to the 1-D numerical model previously discussed, a 2-D model for the distribution of residual stress resulting from the deposition of a single molten droplet is outlined in Chin *et al.* (1996a). The results for the 2-D model of a single deposited droplet on a clamped substrate predict high stress gradients along the droplet centerline, near the top of the droplet. The high stress gradients in the 2-D model result from the traction-free boundaries of the deposited droplet, which reduce the constraint applied to the droplet centerline. Figure 6 depicts representative 2-D numerical results for radial stresses along the centerline of a semi-spherical, stainless steel droplet deposited onto a 0.50 inch thick carbon steel substrate. Note the similarity between the gradients in the measured stresses of Fig. 5 and the gradients in the computed stresses

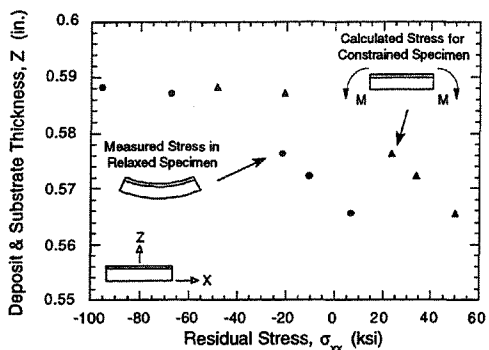


Figure 5. Measured Stress Distribution (Location 1)

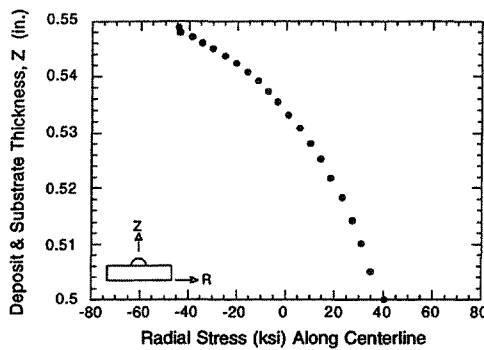


Figure 6. 2-D Model Stress Distribution

of Fig. 6. The numerical results predict stress gradients of -5,700 ksi/in in the top of the droplet and -2,700 ksi/in in the middle of the droplet. The measured stress gradients near the top of the deposit are higher than those predicted by the 2-D model, however the numerical predictions are comparable to the measured stress gradients at greater depths into the deposit. Thus, the stress gradients measured using x-ray diffraction indicate that the droplet-by-droplet nature of the microcasting process is reflected in the stress distributions of fully dense deposits, as was also seen in the warping test results of the previous section. This observation is also in keeping with the findings of Klingbeil and Beuth (1997), in which variations in interfacial fracture toughness were observed in microcast stainless steel/copper interfaces.

Conclusions

In this study, two methods for measuring residual stresses in microcast 308L stainless steel SDM deposits have been outlined. First, techniques for measuring warping in plate-shaped deposits have been described. These techniques are useful in determining gross effects of process changes on residual stress magnitudes, which is the focus of ongoing research. The results discussed in this paper indicate that warping is more severe parallel to the direction of material deposition, and that different material deposition paths might be used to decrease warping in critical directions or to obtain more uniform warping. The measured warping strains and curvatures are significantly lower than those predicted using results from a 1-D thermomechanical numerical model, which is likely a consequence of the droplet-by-droplet nature of the microcasting process. Residual stress measurements have also been obtained by x-ray diffraction. X-ray diffraction measurements have illustrated significant in-plane variations in residual stresses and residual stress gradients as a function of depth into the deposit. Good agreement has been observed between the measured stress gradients and those predicted by 2-D numerical modeling, which strongly suggests that the measured gradients are due to free-edge effects in deposited droplets. Thus, results from both the warping and x-ray diffraction testing suggest that effects of the droplet-by-droplet nature of the microcasting process exist even in fully dense microcast layers.

Acknowledgments

The authors gratefully acknowledge financial support from the Engineering Design Research Center, an Engineering Research Center of the National Science Foundation under Grant EEC-8943164, the National Science Foundation Graduate Research Traineeship Program under Grant EID-9256665 and the Office of Naval Research under Grant 96PR03703-00.

References

- Amon, C.H., Beuth, J.L., Merz, R., Prinz, F.B. and Weiss, L.E., 1997, "Shape Deposition Manufacturing with Microcasting: Processing, Thermal and Mechanical Issues," submitted to the *Journal of Manufacturing Science and Engineering*.
- ASM Metals Handbook*, 1973, Vol. 8, T. Lyman *et al.*, eds., American Society for Metals.
- ASTM Standard E915-90, 1990, *Annual Book of ASTM Standards*, Vol. 03.01, American Society for Testing Materials.
- Chin, R.K., Beuth, J.L., and Amon, C.H., 1996a, "Thermomechanical Modeling of Molten Metal Droplet Solidification Applied to Layered Manufacturing," *Mechanics of Materials*, Vol. 24, pp. 257-271.
- Chin, R.K., Beuth, J.L. and Amon, C.H., 1996b, "Thermomechanical Modeling of Successive Material Deposition in Layered Manufacturing," *Proc. 1996 Solid Freeform Fabrication Symposium* (D.L. Bourell, J.J. Beaman, H.L. Marcus, R.H. Crawford, and J.W. Barlow, eds.), Austin, August 1996, pp. 507-515.
- Chin, R.K., Beuth, J.L. and Amon, C.H., 1995, "Control of Residual Thermal Stresses in Shape Deposition Manufacturing," *Proc. 1995 Solid Freeform Fabrication Symposium* (H.L. Marcus, J.J. Beaman, D.L. Bourell, J.W. Barlow and R.H. Crawford, eds.), Austin, August 1995, pp. 221-228.
- Cullity, B.D., 1978, *Elements of X-Ray Diffraction*, 2nd Edition, Reading, Massachusetts, Addison-Wesley Publishing.
- Fessler, J.R., Merz, R., Nickel, A.H. and Prinz, F.B., 1996, "Laser Deposition of Metals for Shape Deposition Manufacturing," *Proc. 1996 Solid Freeform Fabrication Symposium* (D.L. Bourell, J.J. Beaman, H.L. Marcus, R.H. Crawford, and J.W. Barlow, eds.), Austin, August 1996, pp. 117-124.
- Klingbeil, N.W. and Beuth, J.L., 1997, "Interfacial Fracture Testing of Deposited Metal Layers Under Four-Point Bending," *Engineering Fracture Mechanics*, Vol. 56, No. 1, pp. 113-126.
- Merz, R., Prinz, F.B., Ramaswami, K., Terk, M. and Weiss, L.E., 1994, "Shape Deposition Manufacturing," *Proc. 1994 Solid Freeform Fabrication Symposium* (H.L. Marcus, J.J. Beaman, J.W. Barlow, K.L. Bourell and R.H. Crawford eds.), Austin, August 1994, pp. 1-8.
- Pister, K.S. and Dong, S.B., 1959, "Elastic Bending of Layered Plates," *ASCE Journal of the Engineering Mechanics Division*, Vol. EM 4, pp. 1-10.
- Prinz, F.B., Weiss, L.E., Amon, C.H. and Beuth, J.L., 1995, "Processing, Thermal and Mechanical Issues in Shape Deposition Manufacturing," *Proc. 1995 Solid Freeform Fabrication Symposium* (H.L. Marcus, J.J. Beaman, D.L. Bourell, J.W. Barlow and R.H. Crawford, eds.), Austin, August 1995, pp. 118-129.
- SAE J784a, 1971, *Residual Stress Measurement by X-Ray Diffraction*, prepared by the X-Ray Division of the SAE Fatigue Design and Evaluation Committee, Society of Automotive Engineers, Warrendale, PA.